

## TUTORIAL REVIEW

[View Article Online](#)  
[View Journal](#) | [View Issue](#)



Cite this: *Anal. Methods*, 2024, **16**, 6323

Received 3rd July 2024  
Accepted 10th August 2024

DOI: 10.1039/d4ay01242a  
[rsc.li/methods](http://rsc.li/methods)

## Glowing discoveries: Schiff base-cyanostilbene probes illuminating metal ions and biological entities

Afrin A, Chinna Ayya Swamy P \* and Angel Rose

Schiff bases featuring cyanostilbene units have emerged as versatile and highly effective probes for the selective detection of various metal ions as well as biologically important species. This review comprehensively highlights recent advances in the development and application of the probes, which exhibit remarkable Aggregation-Induced Emission (AIE), Twisted Intramolecular Charge Transfer (TICT), and Excited-State Intramolecular Proton Transfer (ESIPT) properties. These unique structural characteristics facilitate their potential applications in the detection of biologically important metal ions such as  $Zn^{2+}$ ,  $Fe^{3+}$ ,  $Cu^{2+}$ ,  $Hg^{2+}$  and  $Co^{2+}$  ions with high sensitivity and selectivity. Furthermore, these probes have demonstrated significant potential in the recognition of vital biological species, including arginine, hydrazine and hypochlorite ( $ClO^-$ ). The present review discusses the underlying detection mechanisms, emphasizing the role of the Schiff base and cyanostilbene moieties for the selective detection of particular biologically important entities. Moreover, this discussion highlights the practical applications, problems, and future directions in this fast-growing field, emphasizing the vital importance of these probes in both analytical chemistry and bioassays.

## Introduction

Detecting metal ions in environmental and biological systems is crucial due to their significant roles in health and disease.<sup>1</sup> Essential metals such as iron, copper, and zinc are vital for numerous biochemical processes, yet their imbalance can lead to toxicity and various health issues.<sup>2</sup> In contrast, heavy metals such as lead, mercury, and cadmium are toxic even at low concentrations.<sup>3</sup> Therefore, developing probes that are both effective and highly sensitive for metal ion detection is essential for monitoring and managing these ions. Among the various chemical sensors developed, Schiff bases stand out due to their imine ( $=C=N$ ) functional group.<sup>4-11</sup> These compounds are known for their structural versatility, ease of synthesis, and strong affinity for binding with metal ions, making them excellent candidates for sensor development.<sup>12</sup> Schiff bases are synthesized through the condensation of primary amines with carbonyl compounds and can be modified to enhance their electronic properties through different substitutions. Their applications are vast, including roles in catalysis,<sup>13-15</sup> medicinal chemistry,<sup>16,17</sup> and metal ion detection.<sup>18-20</sup> The ability to tailor the Schiff bases to form complex structures enhances their sensitivity and binding properties towards specific metal ions, making them vital tools in this field.

Main Group Organometallics Optoelectronic Materials and Catalysis Lab, Department of Chemistry, National Institute of Technology, Calicut, 673601, India. E-mail: [swamy@nitc.ac.in](mailto:swamy@nitc.ac.in)

Recently, researchers have focused on incorporating cyanostilbene units into Schiff bases for metal ion detection, garnering considerable attention. Cyanostilbene derivatives are noted for their significant photophysical properties, such as twisted intramolecular charge transfer (TICT)<sup>21-23</sup> and aggregation-induced emission (AIE).<sup>24-31</sup> These properties greatly enhance the sensitivity and selectivity of probes, making them highly effective for metal ion detection. TICT facilitates fluorescence changes when metal ions bind, while AIE helps to prevent the common issue of fluorescence quenching in the aggregated state. Combining Schiff bases with cyanostilbene units results in highly responsive probes that exhibit noticeable fluorescence changes upon interacting with specific metal ions. The cyanostilbene moiety, featuring a conjugated system and an electron-withdrawing cyano group, improves the probe's sensitivity and selectivity toward metal ions. The mechanism of metal ion detection, typically involves coordination between the metal ions and the nitrogen or oxygen atoms in the Schiff base. This interaction leads to changes in the electronic properties of the cyanostilbene unit, causing observable fluorescence changes. These changes can be quantified to determine the presence and concentration of metal ions, making these probes highly valuable for analytical and biological applications.

This review provides an extensive overview of recent progress in the development of Schiff bases integrated with cyanostilbene units as fluorescent probes for selective and sensitive detection of biologically important metal ions. The studies collectively highlight the advancements and potential of these



hybrid compounds, demonstrating their high sensitivity and selectivity. We begin by examining the molecular design strategies used to create Schiff base-cyanostilbene compounds. Key approaches include modifying Schiff base structures to improve metal ion binding and integrating cyanostilbene moieties to exploit their distinctive photophysical properties. The resulting structural diversity and tunability of these compounds are essential for optimizing their performance as metal ion sensors. Additionally, the review investigates into the practical applications of these probes, showcasing their effectiveness in detecting various metal ions such as  $Zn^{2+}$ ,  $Cu^{2+}$ ,  $Fe^{3+}$ , and  $Hg^{2+}$ , along with other significant species like hydrazine,  $ClO^-$ , arginine. These examples underscore the versatility and practical utility of Schiff base-cyanostilbene probes in environmental and biological contexts. We also address the challenges faced in developing and applying these probes, including issues of stability, selectivity in complex environments, and the necessity for real-time and on-site detection capabilities. The review concludes with a forward-looking perspective, suggesting potential enhancements and innovations to further improve the performance and expand the applicability of Schiff base-cyanostilbene probes.

### The versatility of Schiff base-based probes in metal ion detection: synthesis, tunability, and applications

Schiff bases, first synthesized by Hugo Schiff in 1864, are characterized by the presence of an azomethine group ( $-C=N-$ ).<sup>32</sup> These compounds have garnered significant attention in various fields, particularly in the development of probes for metal ion detection.<sup>33-35</sup> The versatility of Schiff base-based probes stems from their facile synthesis, structural flexibility, tunable properties, and strong coordination ability with metal ions, making them indispensable in analytical chemistry. One of the primary advantages of Schiff bases is their ease of synthesis, involving the condensation reaction between a primary amine and carbonyl compounds (usually aldehydes or ketones) to form an imine linkage ( $-C=N-$ ) (Fig. 1). This reaction generally takes place under mild conditions, often with the aid of a dehydrating agent to remove the water produced during the process. This simple method allows for the rapid generation of a wide range of Schiff bases with diverse functional groups, enabling the fine-tuning of their chemical and physical properties. The azomethine group in Schiff bases is particularly effective as a ligand for coordinating with metal ions. The nitrogen atom in the imine linkage, along with other donor atoms such as oxygen or sulfur in the Schiff base structure, can form stable complexes with different metal ions, enhancing the probe's sensitivity and allowing for the detection of metal ions at very low concentrations. Furthermore, the formation of these complexes often leads to notable changes in the probe's optical properties, such as shifts in absorption or emission spectra,



Fig. 1 General synthetic representation of Schiff bases.

which can be easily tracked using spectroscopic techniques. The structural versatility of Schiff bases is crucial in designing probes for specific metal ions, as even minor structural modifications can greatly influence their selectivity and sensitivity. Schiff bases are highly adaptable in their photophysical and chemical properties. By altering the substituents on the amine or carbonyl components, researchers can adjust the electronic characteristics of the azomethine bond, affecting the probe's fluorescence, colorimetric response, and binding affinity towards metal ions. This adaptability is crucial for creating highly selective probes capable of differentiating between various metal ions in complex environments, which is particularly valuable in environmental monitoring, clinical diagnostics, and industrial applications.

### Cyanostilbene derivatives: enhancing optoelectronics through unique properties

Compounds featuring cyanostilbene units have become significant components in the field of organic materials and optoelectronics, primarily due to their unique photophysical properties and versatile applications.<sup>36</sup> These compounds, characterized by a distinctive twisted structure with a cyano group attached to a stilbene core, exhibit remarkable features that make them valuable in various areas. One of the most distinguished characteristics of cyanostilbene units is their exceptional photophysical properties. They exhibit strong fluorescence and high quantum yields in the solid state, making them excellent candidates for optoelectronic devices and fluorescence-based applications.<sup>37</sup> Cyanostilbene units attached to donor moieties such as carbazole,<sup>38-40</sup> triphenylamine,<sup>41,42</sup> tetraphenylethene,<sup>43,44</sup> and so on are particularly notable for their significant solvatochromism, where their emission color changes with the polarity of the solvent. This phenomenon is utilized in designing molecular sensors that can detect environmental changes by altering their fluorescence in response to different stimuli. The structural versatility of cyanostilbene units allows for extensive modifications, enabling the design of molecules with fine-tunable properties. The stilbene core can be functionalized with various substituents, altering the electronic and steric properties of the molecule. This design flexibility is crucial for developing new materials with specific characteristics, such as improved stability, solubility, or enhanced interaction with other molecules or surfaces. The ability to fine-tune their photophysical properties through chemical modifications further enhances the utility of cyanostilbene in various applications. In summary, cyanostilbene units' unique combination of strong fluorescence, high quantum yields, solvatochromism, and structural versatility makes them vital in the development of advanced materials for optoelectronic and sensing applications.<sup>45,46</sup>

### Advancements on Schiff-base with cyanostilbene conjugates

In 2014, Zhang *et al.* were the first to discover a novel Schiff base incorporating a cyanostilbene unit probe **1**, for the selective detection of  $Hg^{2+}$  ions with aggregation-induced emission enhancement (AIEE) properties in  $THF/H_2O$  mixtures (Fig. 2).<sup>47</sup>



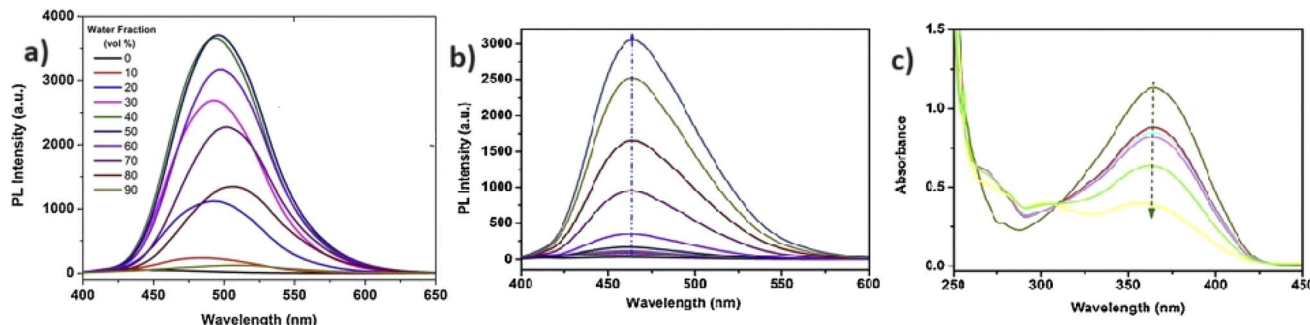
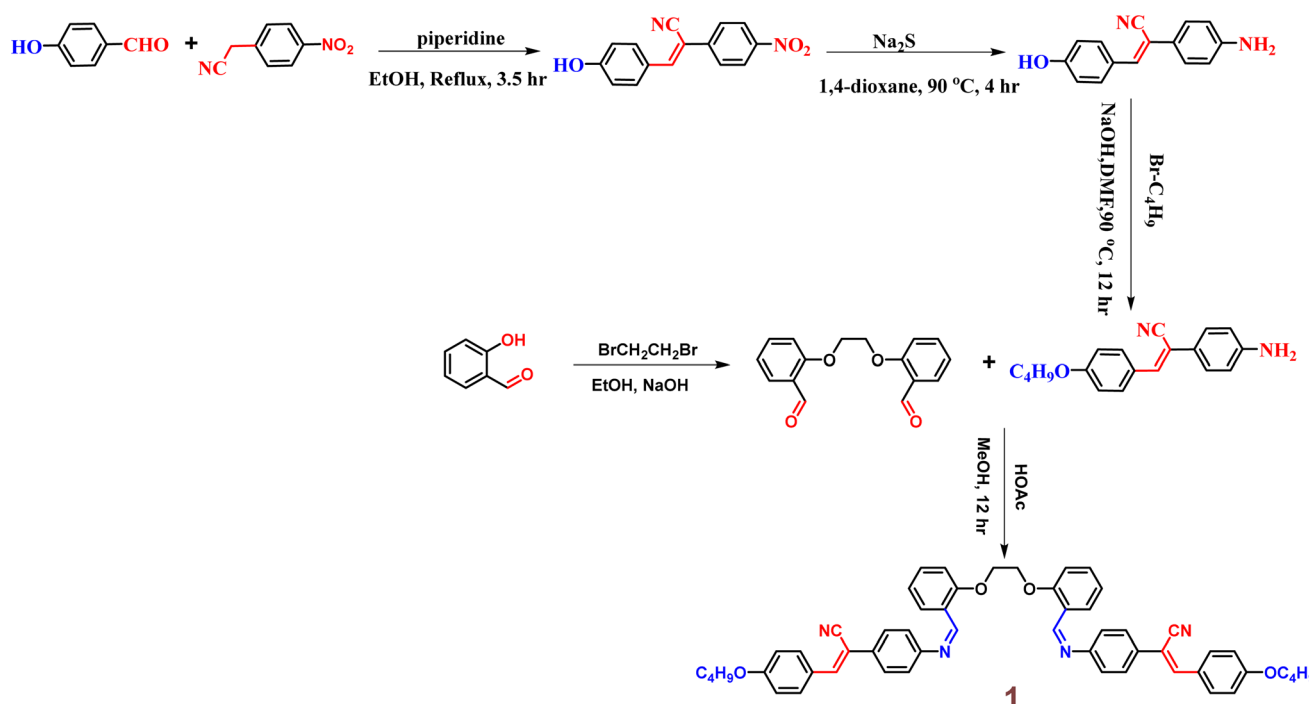


Fig. 2 (a) Emission spectra of probe **1** in THF–H<sub>2</sub>O mixtures; (b) change in the emission spectra of **1** upon increasing the concentrations of Hg<sup>2+</sup> ions in THF; (c) absorption spectra of **1** upon increasing concentrations Hg<sup>2+</sup> ions in THF. Reproduced with permission from ref. 47. Copyright 2014 Elsevier.

The probe **1** was developed by following simple synthetic pathway as depicted in the Scheme 1. This tweezer-shaped **1** detects Hg<sup>2+</sup> ions through a fluorescence *turn-on* response due to a configuration change and/or the formation of intermolecular aggregates. The selectivity of **1** towards Hg<sup>2+</sup> ions were also confirmed by the UV-vis as well as fluorescence titration studies (Fig. 2). The binding ability of **1** with Hg<sup>2+</sup> ions were further confirmed by <sup>1</sup>H NMR spectroscopy. The Job's plot analysis revealed a 1:1 binding stoichiometry between **1** and Hg<sup>2+</sup> ions. The association constant (*K*) and detection limit estimated by the Benesi–Hilderbrand equation as  $1.5 \times 10^5 \text{ M}^{-1}$  and  $2.4 \times 10^{-5} \text{ M}$ , respectively. The competitive binding studies in the presence of various metal ions showed no significant changes, thereby emphasizing the high selectivity of **1** towards Hg<sup>2+</sup> ions even in the presence of other metal ions.

In the same year, the research group subsequently designed and synthesized a novel Schiff-base featuring an  $\alpha$ -cyanostilbene unit **2**, aimed at the selective detection of Zn<sup>2+</sup> ions under physiological conditions.<sup>48</sup> The sensing studies strongly suggested that the probe **2** effectively distinguishes Zn<sup>2+</sup> ions from Cd<sup>2+</sup> and Hg<sup>2+</sup> ions (Fig. 4). The Job's plot demonstrated a binding ratio of 1:1 for **2** and Zn<sup>2+</sup> ions. The association constant and detection limit of **2** with Zn<sup>2+</sup> were determined using the Benesi–Hilderbrand equation and calculated to be  $2.317 \times 10^5 \text{ M}^{-1}$  and 0.1  $\mu\text{M}$ , respectively. The fluorescence *turn-on* sensing mechanism of probe **2** for Zn<sup>2+</sup> ions is primarily attributed to the restriction of C=N isomerization, which results in a chelation-enhanced fluorescence (CHEF) effect (Fig. 3). Upon binding with Zn<sup>2+</sup> ions, the C=N bond's rotational freedom is significantly reduced, leading to an enhanced



Scheme 1 Synthesis pathway adapted for the synthesis of **1**.



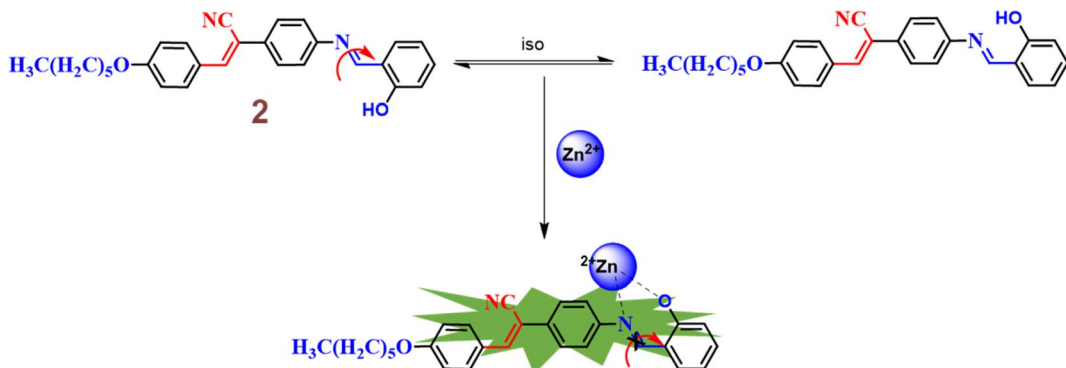
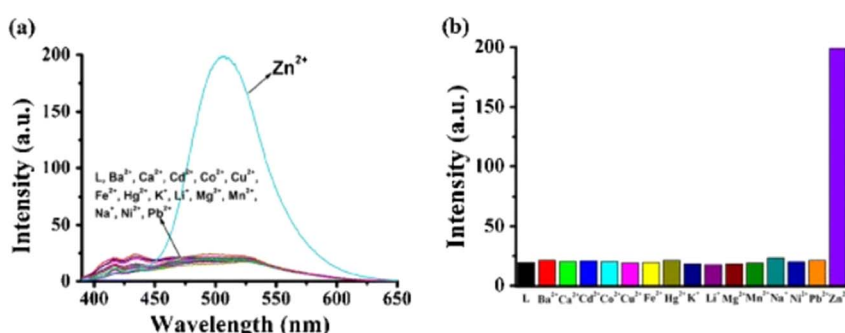
Fig. 3 Proposed sensing mechanism of 2 with  $Zn^{2+}$  ions.

Fig. 4 (a) Emission spectra of probe 2 alone and with different metal ions. (b) Fluorescent intensity of 2 at 509 nm with different metal ions. Reproduced with permission from ref. 48. Copyright 2014 Springer.

fluorescence signal. This restriction prevents non-radiative decay pathways, allowing for a more efficient radiative emission, thus intensifying the fluorescence. The CHEF effect is a common phenomenon in metal ion sensing, where the coordination of the metal ion stabilizes the molecular structure and enhances the fluorescent properties of the sensor. Further, the probe 2 demonstrated a strong response towards the  $Zn^{2+}$  ions over a pH range of 6–12. In contrast, at pH 1 to 5, the fluorescence intensity was weak and gradually decreased with lower pH levels. This results strongly suggests that the sensing behavior of 2 towards  $Zn^{2+}$  ions is effective in alkaline, neutral, and mildly acidic conditions.

In 2015, authors combined a coumarin unit with a cyanostilbene-containing Schiff base to design and synthesize probe 3 (Fig. 5), which exhibits selective detection of  $Hg^{2+}$  ions over other competitive metal ions.<sup>49</sup> The probe 3 exhibited excellent AIEE ability due to the synergistic effect of intramolecular polarization of the  $\alpha$ -cyanostilbene unit and the formation of excimers between molecular dimers. The nitrogen and oxygen

atoms in the structure provide binding sites for  $Hg^{2+}$  coordination, leading to the aggregation of probe 3 and resulting in a fluorescence *turn-on* response (Fig. 6). The coordination with  $Hg^{2+}$  ions induces molecular aggregation, which restricts intramolecular rotations and vibrations, thereby enhancing the fluorescence emission through the AIEE mechanism. This probe has proven to be effective for detecting  $Hg^{2+}$  in both aqueous environments and *in vivo* biological systems (Fig. 6). In 2016, the same team designed another AIE-active probe, probe 4 (Fig. 5), featuring a linear conjugated bis-Schiff base for the selective detection of  $Hg^{2+}$  ions (Fig. 7).<sup>50</sup> The unique color shifts and fluorescence emission of  $Hg^{2+}$  ions in THF and THF/H<sub>2</sub>O mixtures provided a quick and simple method for discriminating  $Hg^{2+}$  ions using the naked eye or a UV lamp. Probe 4 exhibited a low limit of detection of  $3.4 \times 10^{-9}$  M in THF and  $2.4 \times 10^{-7}$  M in THF/H<sub>2</sub>O, demonstrating high sensitivity and selectivity for  $Hg^{2+}$  ions through a fluorescence *turn-on* response. Moreover, probe 4 shows potential for the detection of  $Hg^{2+}$  ions in living cells as well as in THF and THF/H<sub>2</sub>O mixtures.

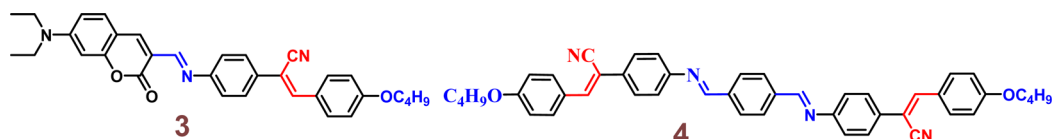


Fig. 5 Chemical structures of probes 3 and 4.



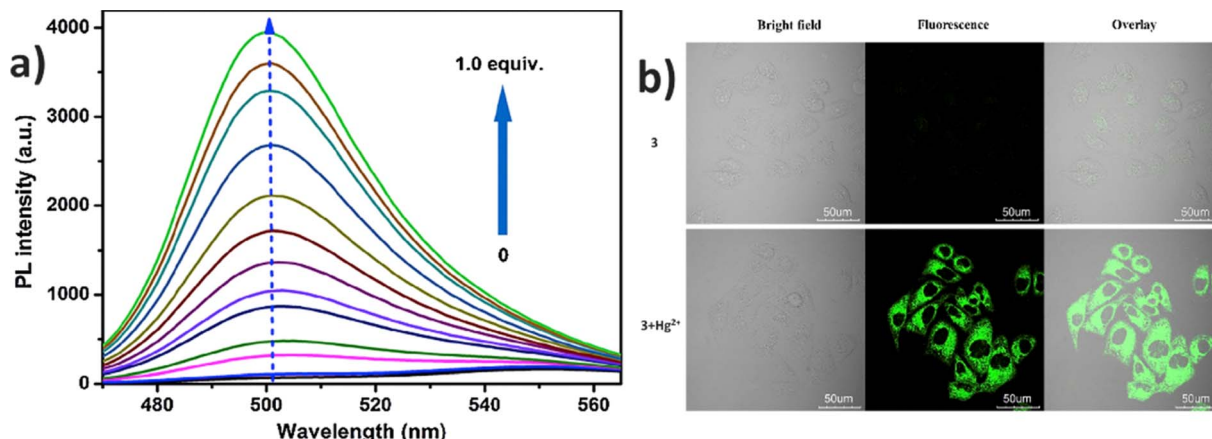


Fig. 6 (a) Emission spectra of probe 3 with increasing concentrations of  $\text{Hg}^{2+}$  ions in a DMSO/H<sub>2</sub>O ( $f_w = 20\%$ ) mixture; (b) fluorescence images of HeLa cells treated with 3 and  $\text{Hg}^{2+}$  ions. Reproduced with permission from ref. 49. Copyright 2015 Elsevier.

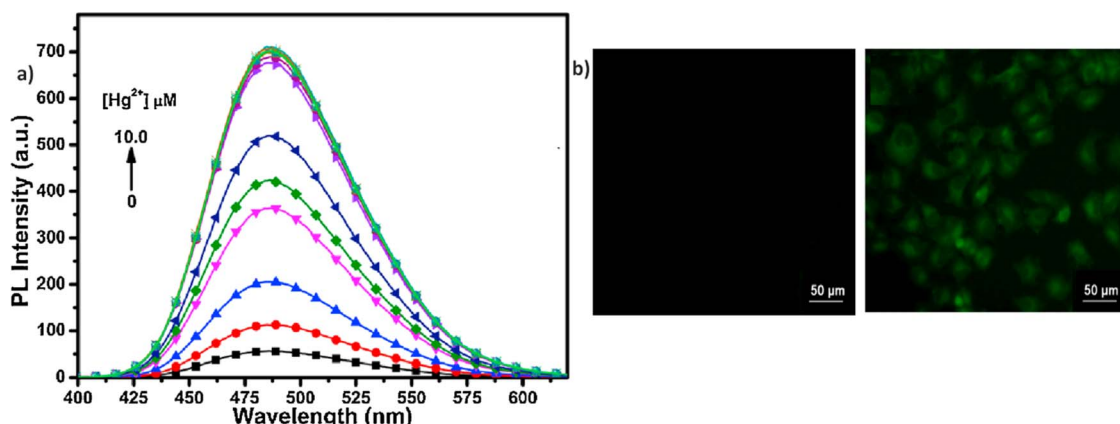


Fig. 7 (a) Emission spectra of probe 4 with increasing concentrations of  $\text{Hg}^{2+}$  ions in a DMSO/H<sub>2</sub>O ( $f_w = 20\%$ ) mixture; (b) fluorescence images of HeLa cells treated with 4 and  $\text{Hg}^{2+}$  ions. Reproduced with permission from ref. 50. Copyright 2016 Elsevier.

$\text{H}_2\text{O}$ , showcasing its versatility and practical application in various environments (Fig. 7).

In 2021, Yang *et al.* developed a highly sensitive fluorescent receptor, probe 5, designed for the detection of  $\text{ClO}^-$  ions in aqueous media, which based on a thiophene-cyanostilbene conjugated Schiff base.<sup>51</sup> Probe 5 exhibited strong fluorescence quantum yields as prepared and demonstrated selective detection of  $\text{ClO}^-$  ions, even in the presence of other competing species, with a fluorescence *turn-off* response (Fig. 9). The limit of detection (LOD) for  $\text{ClO}^-$  was determined to be  $3.2 \times 10^{-8} \text{ M}$ . The sensing mechanism was validated using FT-IR spectroscopy, fluorescence Job's plot, <sup>1</sup>H NMR spectroscopy, and mass spectrometry. The study revealed that  $\text{ClO}^-$  oxidizes the sulfur

in the thiophene unit of probe 5 (Fig. 8). This oxidation reaction significantly alters the electronic properties of the thiophene unit, leading to a detectable change in the fluorescence signal of the probe. The specific interaction between  $\text{ClO}^-$  and the sulfur atom in the thiophene ring provides a selective and sensitive mechanism for detecting  $\text{ClO}^-$  ions, the probe 5 was successfully applied to detect  $\text{ClO}^-$  in real samples and for living-cell imaging, highlighting its potential for *in vitro* assays and environmental monitoring of  $\text{ClO}^-$  ions (Fig. 9). This study underscores the versatility and efficacy of probe 5 in practical applications, offering a valuable tool for both environmental detection and biological research.

The following year, the same research group developed another biphenyl-cyanostilbene conjugate Schiff base dual sensor (probe 6) for the simultaneous detection of  $\text{Cu}^{2+}$  and  $\text{Zn}^{2+}$  ions.<sup>52</sup> This probe features long-wavelength fluorescence in the 550–750 nm range in aqueous media, with a fluorescence *turn-off* response for  $\text{Cu}^{2+}$  ions and a ratiometric response for  $\text{Zn}^{2+}$  ions (Fig. 10). Additionally, probe 6 exhibited an excellent selective colorimetric response towards  $\text{Zn}^{2+}$  ions, changing from red to yellow. The detection of  $\text{Cu}^{2+}$  and  $\text{Zn}^{2+}$  ions were

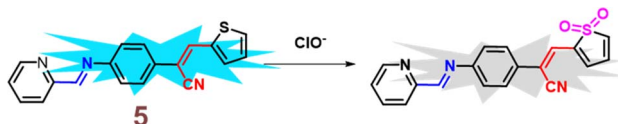


Fig. 8 Proposed sensing mechanism of 5 with  $\text{ClO}^-$  ions.

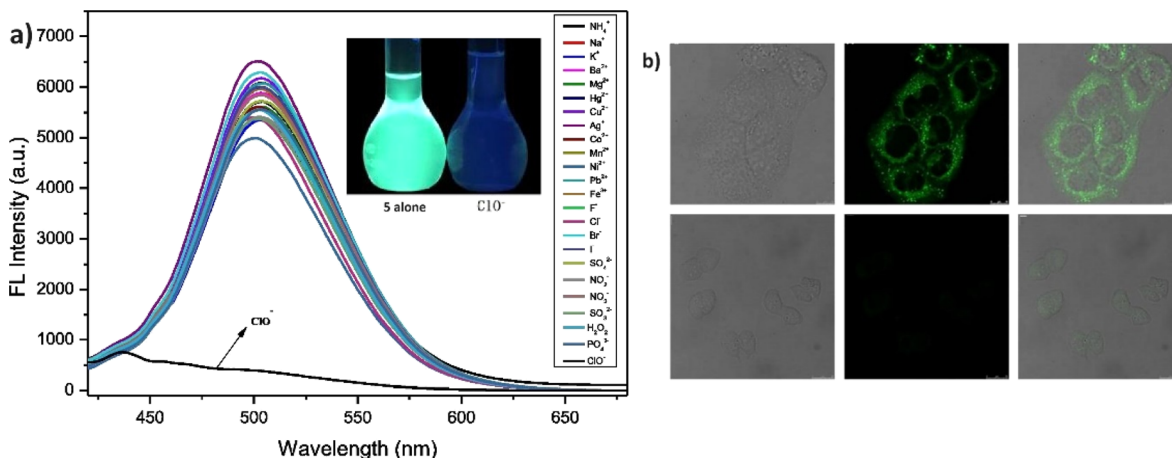


Fig. 9 (a) Emission spectra of probe 5 with increasing concentrations of  $\text{ClO}^-$  ions in a THF/H<sub>2</sub>O mixture; (b) confocal fluorescence images of MCF-7 cells treated with probe 5 and probe 5 with  $\text{ClO}^-$  ions MCF-7 cells with probe 5 alone (top) MCF-7 cells with 5 +  $\text{ClO}^-$  (bottom). Reproduced with permission from ref. 51. Copyright 2021 Elsevier.

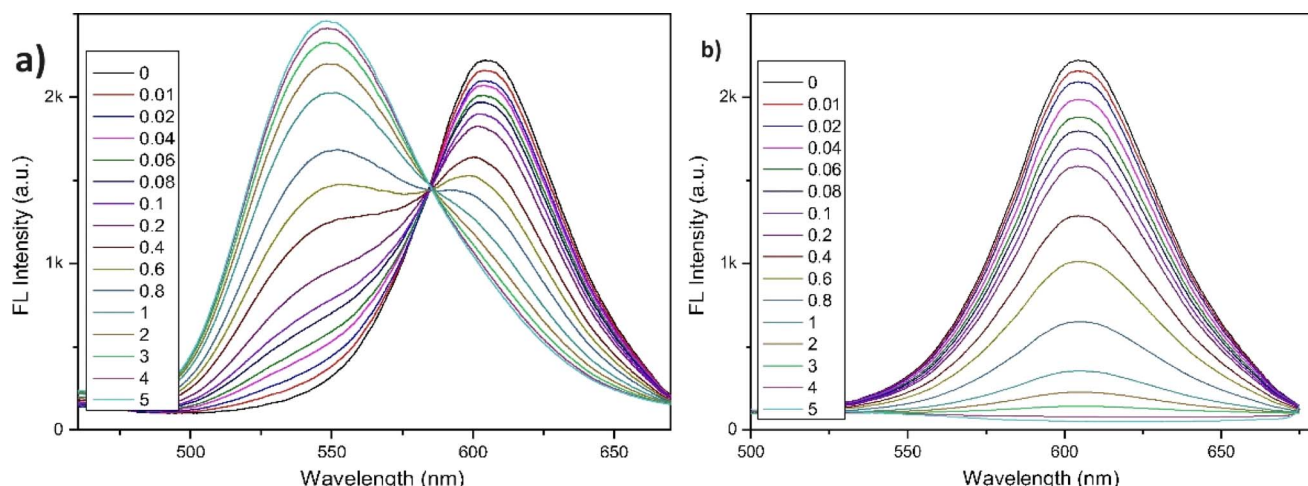


Fig. 10 (a) Fluorescence spectra of probe 6 with different concentrations of  $\text{Zn}^{2+}$  in THF/H<sub>2</sub>O (b) fluorescence spectra of probe 6 with different concentrations of  $\text{Cu}^{2+}$  ions in THF/H<sub>2</sub>O. Reproduced with permission from ref. 52. Copyright 2022 Elsevier.

achieved without mutual interference in their coexistence system, facilitated by the presence of ATP. The detection limits for  $\text{Cu}^{2+}$  and  $\text{Zn}^{2+}$  ions were determined to be  $2.3 \times 10^{-7}$  M and  $1.8 \times 10^{-6}$  M, respectively. Furthermore, probe 6 demonstrated strong bioimaging performance and *in situ* sensing capabilities for  $\text{Cu}^{2+}$  and  $\text{Zn}^{2+}$  ions in living cells, indicating its potential for detecting these ions in both *in vitro* tests and *in vivo* environments (Fig. 11). This dual sensor offers a valuable tool for the simultaneous monitoring of these metal ions in complex biological and environmental samples, showcasing its versatility and efficacy in practical applications.

They have developed two novel fluorescent liquid crystals based on thiophene-vinyl nitrile Schiff-base derivatives, 7 and 8, which differ in the number of alkyl chains (Fig. 12).<sup>53</sup> Both probes exhibited smectic phases, with phase transition temperatures ranging from 91.5 to 130.6 °C for 7 and from 71.3 to 120.2 °C for 8. They displayed excellent fluorescence in the

aggregated states of the mesophase and solid film, with absolute fluorescence quantum yields of 0.64 and 0.76, respectively, in the solid film. The numerous alkyl chains on these derivatives contributed to their low mesophase transition temperatures and high fluorescence. This study presents the first example of thiophene-containing AIE fluorescent liquid crystals.

Zhu and co-workers designed a new Schiff base probe 9 composed of salicylaldehyde-analogue  $\alpha$ -cyanostilbene and benzophenone hydrazone which emits red fluorescence in 2022 (Fig. 13).<sup>54</sup> The enhanced red emission for probe 9 is due to the combined effects of ESIPT and AIE. ESIPT facilitates a proton transfer in the excited state, resulting in red-shifted emission, while AIE restricts molecular motions in the aggregated state, enhancing fluorescence. Together, these effects lead to a significantly intensified red emission. In the THF/H<sub>2</sub>O system, the probe's highly sensitive and the selective chelating ability

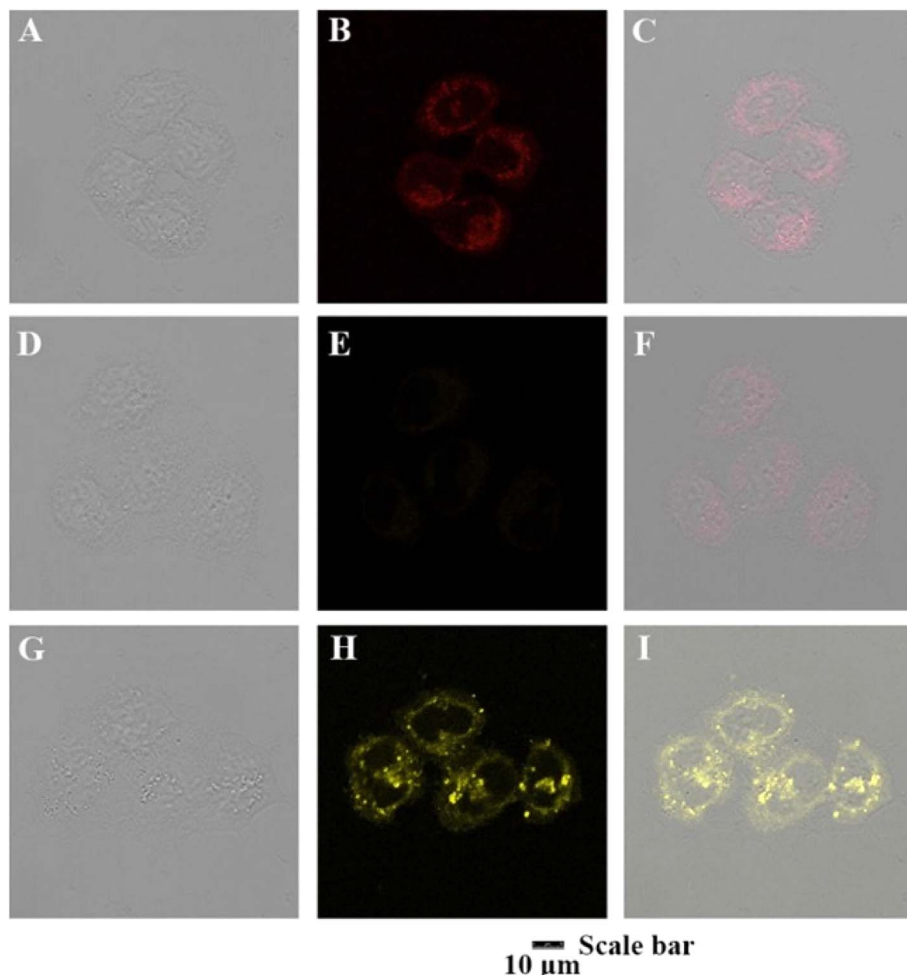


**Fig. 11** Confocal fluorescence images for the living MCF-7 cells in the presence of probe 6, probe 6 + Cu<sup>2+</sup> and probe 6 + Zn<sup>2+</sup> ( $1.0 \times 10^{-5}$  M, each), respectively. (A)–(C) Cells with probe 6; (D)–(F) cells with probe 6 + Cu<sup>2+</sup>; (G)–(I) cells with probe 6 + Zn<sup>2+</sup>. Reproduced with permission from ref. 52. Copyright 2022 Elsevier.

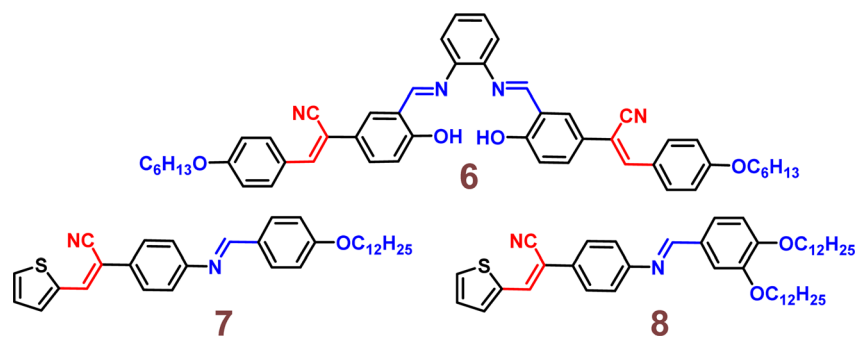


Fig. 12 Chemical structures of probes 6–8.

towards  $\text{Cu}^{2+}$  ions were demonstrated. The probe **9** senses  $\text{Cu}^{2+}$  ions with a fluorescence *turn-off* behavior with detection value of  $2.34 \times 10^{-8}$  M (Fig. 14). The probe **9** has been effectively applied to detect  $\text{Cu}^{2+}$  ions in ambient water samples. The fluorophore-infused silica gel test strip was employed for the spot observation of  $\text{Cu}^{2+}$  under UV light, suggesting the receptors feasible use for visible  $\text{Cu}^{2+}$  ions sensing (Fig. 14).

Yang *et al.* introduced a first fluorescence sensor for hydrazine ion based on thiophene-cyanodistyrene Schiff-base (**10**) in the year 2022.<sup>55</sup> The probe **10** demonstrated weak fluorescence at 450–550 nm in aqueous media as a result of the strong PET effect, which attenuates the AIE effect. However, by interfering with the PET effect (Fig. 15), it demonstrated a high fluorescence *turn-on* response and selective sensing capabilities for

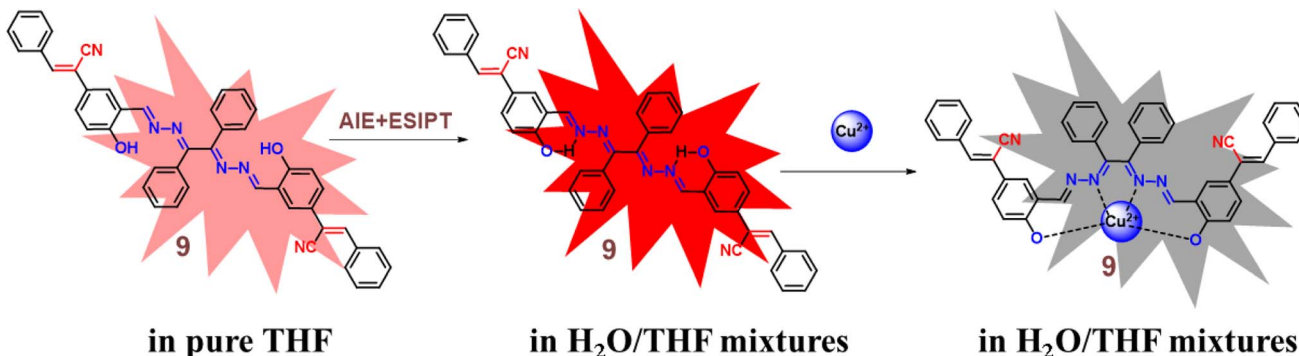


Fig. 13 Chemical structure of probe 9 and the proposed mechanism of probe 9 with Cu<sup>2+</sup> ions.

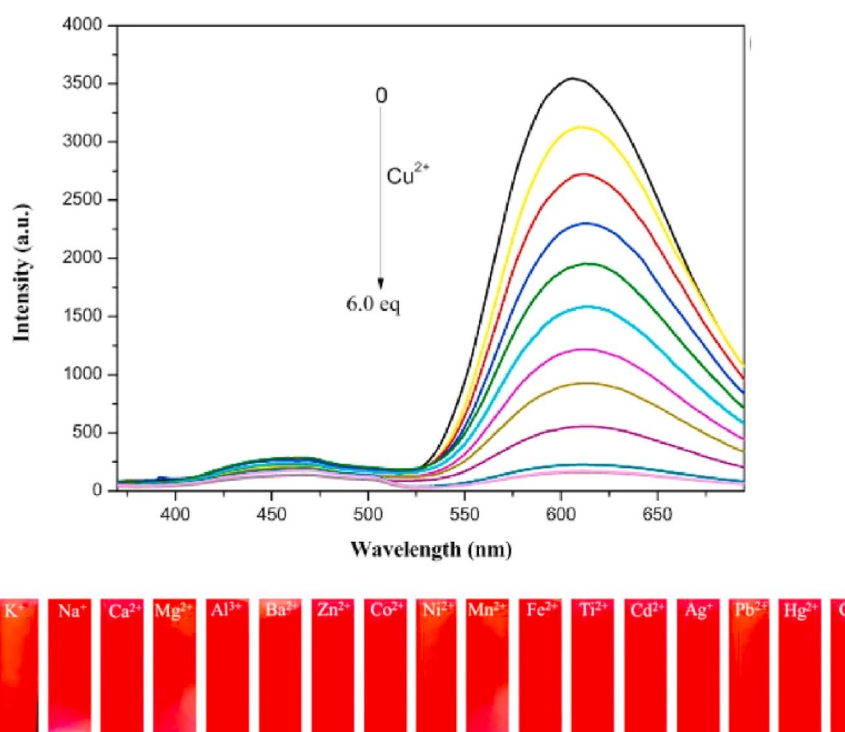


Fig. 14 Emission spectra of probe 9 upon increasing concentrations of Cu<sup>2+</sup> ions in THF/H<sub>2</sub>O mixtures (v/v = 1:9, pH = 7.4,  $\lambda_{\text{ex}} = 350$  nm) (top) and photographs of the silica gel testing strips for detecting various ions including under UV 365 nm illumination (bottom). Reproduced with permission from ref. 54. Copyright 2022 Elsevier.

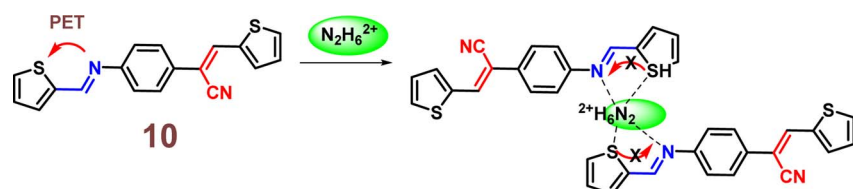


Fig. 15 Proposed sensing mechanism of 10 with N<sub>2</sub>H<sub>6</sub><sup>2+</sup> ions.

Hg<sup>2+</sup> and N<sub>2</sub>H<sub>6</sub><sup>2+</sup> (Fig. 16). Notably, the presence of Cl<sup>-</sup> covered the fluorescence response to Hg<sup>2+</sup>, allowing for the extremely selective detection of N<sub>2</sub>H<sub>6</sub><sup>2+</sup> alone with **10**. The detection limit of **10** for N<sub>2</sub>H<sub>6</sub><sup>2+</sup> ions was established to be  $1.05 \times 10^{-7}$  M. The binding ratio of **10** with N<sub>2</sub>H<sub>6</sub><sup>2+</sup> ions were calculated to be 2:1

which was verified by Job's plot, MS spectrum, <sup>1</sup>H NMR spectrum, FT-IR spectrum, and theoretical computations. The experiment conducted using the probe **10** in tap water and Minjiang River water demonstrated significant potential for sensing N<sub>2</sub>H<sub>6</sub><sup>2+</sup> in real water environments.



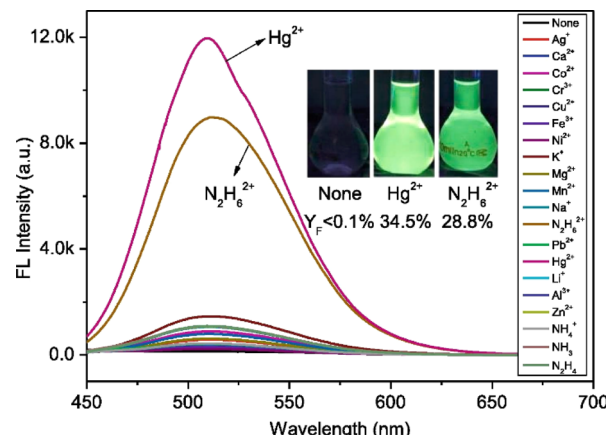


Fig. 16 Fluorescence spectra of probe 10 with different cations. Reproduced with permission from ref. 55. Copyright 2022 Elsevier.

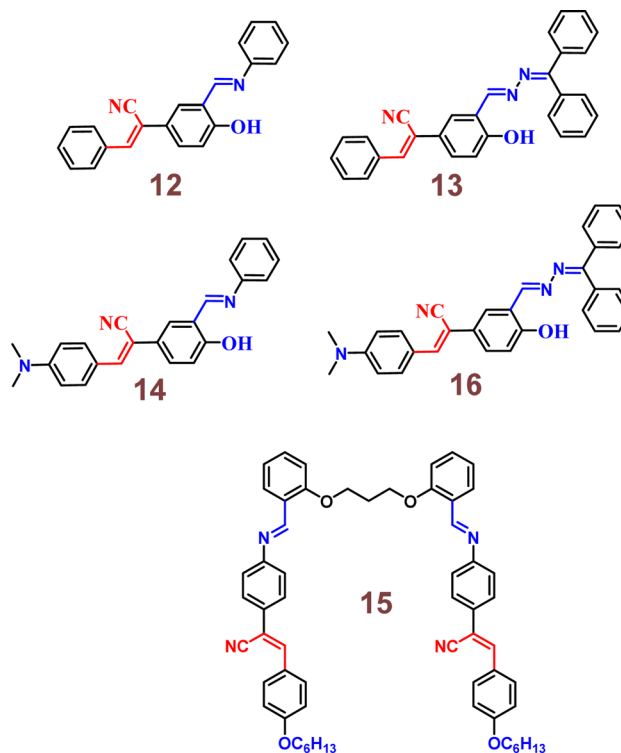


Fig. 19 Chemical structure of probe 12–16.

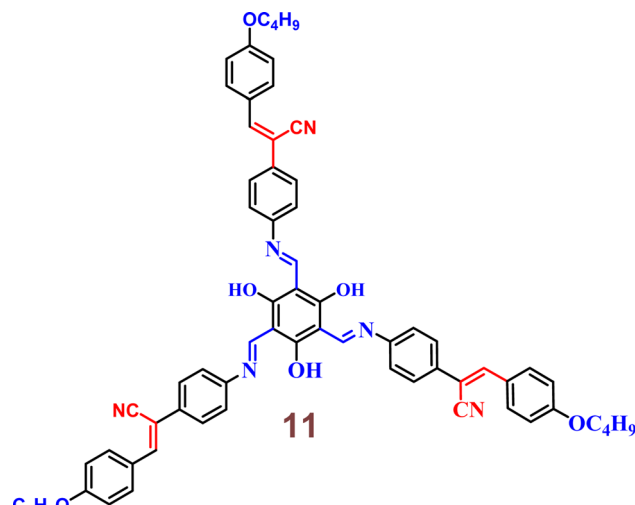


Fig. 17 Chemical structure of probe 11.

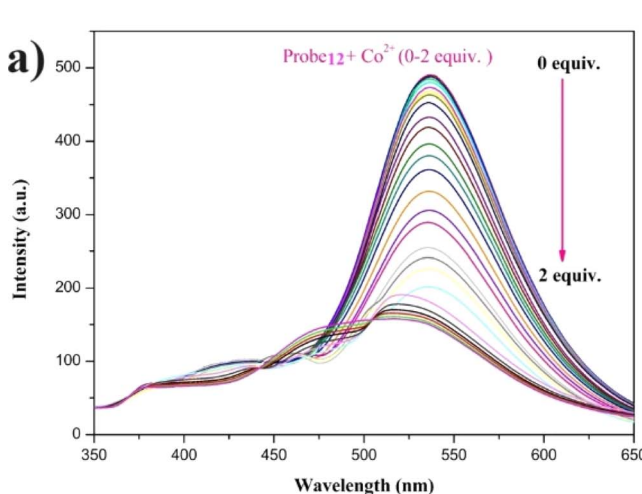
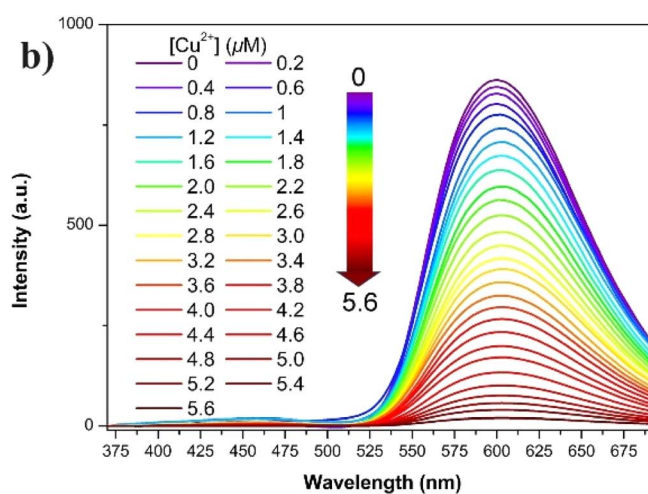


Fig. 18 (a) Emission spectra of probe 12 upon increasing concentrations of  $\text{Co}^{2+}$  ions in  $\text{THF}/\text{H}_2\text{O}$  mixtures ( $f_w = 60\%$ ,  $\text{pH} = 7.4$ ,  $\lambda_{\text{ex}} = 330 \text{ nm}$ ). (b) Emission spectra of probe 13 with increasing  $\text{Cu}^{2+}$  ions concentration in  $\text{THF}/\text{H}_2\text{O}$  ( $f_w = 90\%$ ,  $\text{pH} = 7.4$ ,  $\lambda_{\text{ex}} = 350 \text{ nm}$ ). Reproduced with permission from ref. 57. Copyright 2023 Springer.



because of its high thermal stability and beneficial fluorescence emission.

In 2022, Zhu *et al.* synthesized a salicylaldehyde-functionalized Schiff base with an  $\alpha$ -cyanostilbene unit (probe **12**) for the selective detection of  $\text{Co}^{2+}$  ions.<sup>57</sup> Probe **12** exhibited exceptional AIE and ESIPT emission properties in solution, aggregation, and solid states. The probe **12** displayed distinct fluorescence with varying morphologies when crystallized in pure ethanol or mixtures of ethanol and water (1/2, v/v). For  $\text{Co}^{2+}$  ion sensing, probe **12** demonstrated clear spectroscopic fluorescence quenching of its strong green fluorescence in a THF/ $\text{H}_2\text{O}$  mixture (Fig. 18). The limit of detection for  $\text{Co}^{2+}$  ions was determined to be  $0.41 \times 10^{-8}$  M, with a binding ratio of 2:1. Additionally, probe **12** proved effective for sensing  $\text{Co}^{2+}$  ions in real water samples and on silica gel testing strips, showcasing its practical application in environmental monitoring.

In 2023, the same research group developed a new sensor, probe **13**, specifically tailored for the selective detection of  $\text{Cu}^{2+}$  ions.<sup>58</sup> This innovative probe incorporates a benzophenone hydrazone unit, replacing the phenyl unit found in its predecessor, probe **12**. Probe **13** emitted red fluorescence at 602 nm, attributed to the combined effects of ESIPT and AIE. In the THF/

$\text{H}_2\text{O}$  system, probe **13** demonstrated highly sensitive and selective chelating ability towards  $\text{Cu}^{2+}$  ions, evidenced by the observable fading of red fluorescence with a detection limit of  $2.34 \times 10^{-8}$  M (Fig. 18). Job's plot analysis suggested a 2:1 binding ratio of probe **13** with  $\text{Cu}^{2+}$  ions. Furthermore, probe **13** was effectively applied to detect  $\text{Cu}^{2+}$  ions in ambient water samples. Utilizing probe-permeated silica gel test strips allowed for spot observation of  $\text{Cu}^{2+}$  under UV light, indicating its practical potential for visible  $\text{Cu}^{2+}$  sensing.

Later in the same year, probe **14** was designed, differing from probe **12** by the addition of a dimethylamino group (Fig. 19).<sup>59</sup> Harnessing the synergistic mechanisms of AIE, ESIPT, and ICT, probe **14** exhibited red fluorescence emission at 627 nm in THF/ $\text{H}_2\text{O}$  mixtures (Fig. 20). This probe **14** found effectiveness in various applications, particularly demonstrated through TLC-based test strips loaded with probe **14**. These strips exhibited a reversible fluorescence response to amine/acid vapors and a sensitive, selective fluorescence response to  $\text{Cu}^{2+}$  ions (Fig. 20). Fluorescence titration experiments conducted between probe **14** and  $\text{Cu}^{2+}$  in THF/ $\text{H}_2\text{O}$  mixtures revealed a detection limit of  $1.18 \times 10^{-7}$  M and a binding constant of  $1.59 \times 10^5$ . Job's plot experiments and HR-MS analysis confirmed a 2:1 binding stoichiometry between probe **14** and

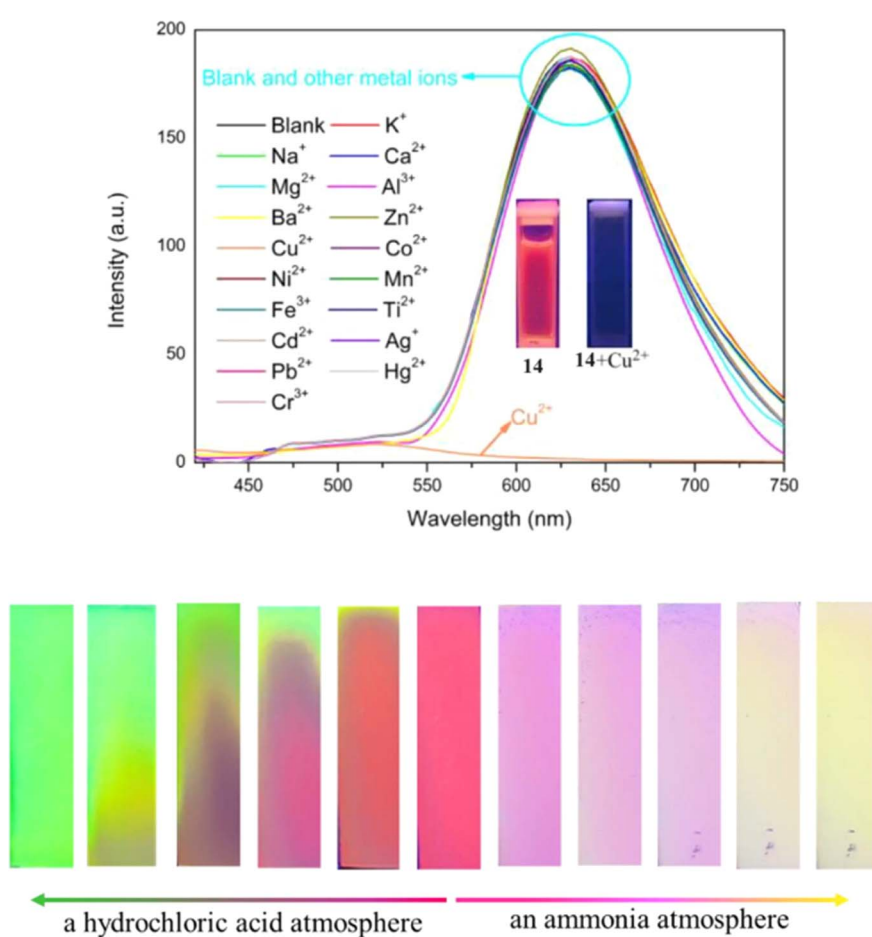


Fig. 20 Emission spectra changes of probe **14** in the presence of various metal cations (in THF/ $\text{H}_2\text{O}$  system ( $f_w = 95\%$ , pH = 7.4,  $\lambda_{\text{ex}} = 400$  nm)) (top); fluorescence color responses of the TLC-based test strips loaded with probe **14** after exposure to HCl and  $\text{NH}_3$  vapors for different times (bottom). Reproduced with permission from ref. 59. Copyright 2023 Elsevier.



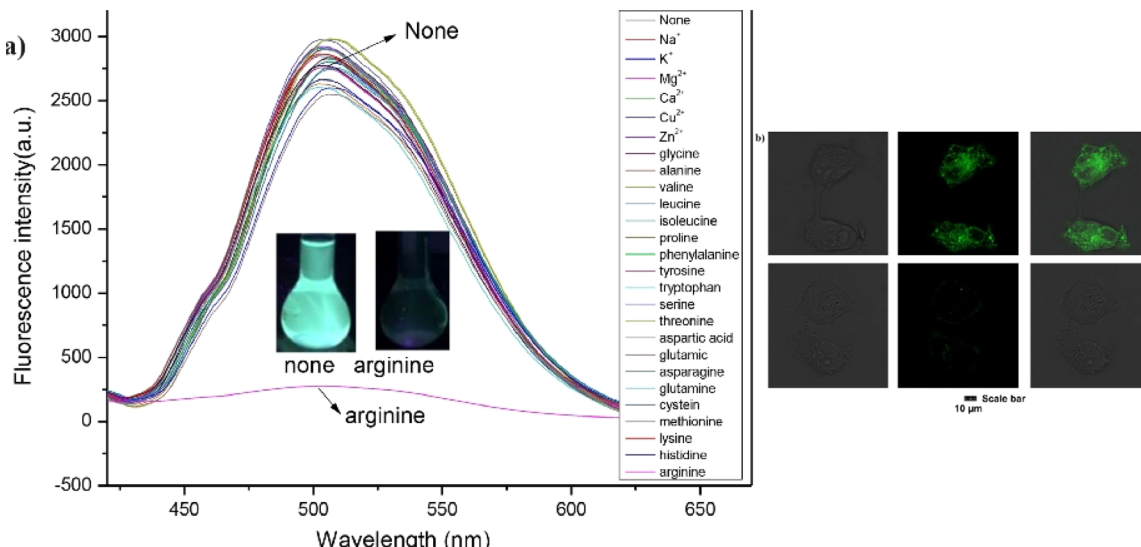


Fig. 21 (a) Fluorescence spectra of probe **15** in the presence of various metal ions and amino acids THF/H<sub>2</sub>O system (b) fluorescence images of MCF-7 cells with probe **15** with arginine. Reproduced with permission from ref. 60. Copyright 2024 Elsevier.

Cu<sup>2+</sup>. This probe enabled real-time assessment of Cu<sup>2+</sup> in actual water samples, providing valuable insights into the development of long-wavelength emissive luminogens based on  $\alpha$ -cyanostilbene.

Yang and co-workers synthesized a fluorescence sensor for arginine based on bis-cyanodistyrene Schiff-base probe (**15**) in 2024.<sup>60</sup> This probe **15** showed high fluorescence in aqueous media and selective sensing property for arginine with a limit of detection of  $1.34 \times 10^{-7}$  M. The multiple intermolecular hydrogen bonds provided an explanation for the binding mechanism. The selective sensing ability of **15** for arginine was successfully demonstrated on test paper and in sample analyses of Minjiang River water and adult urine. The probe **15** was further employed in living-cell imaging experiments, showcasing its excellent fluorescence imaging properties and strong detection capabilities for arginine in a cellular environment (Fig. 21). This research provides an effective method for real-time and *in situ* sensing of arginine in complex environments and living organisms, offering significant potential for practical applications in biochemical and medical fields.

Very recently, in 2024, Zhu and colleagues developed a new Schiff base designated as **16**, which incorporates an electron-donating dimethylamino unit, building upon the design of probe **13**.<sup>61</sup> This probe **16** senses Fe<sup>3+</sup> ions with a decrease in fluorescence intensity and exceptional AIE in THF/H<sub>2</sub>O mixtures (Fig. 22). The limit of detection and the binding constant ( $K_a$ ) values calculated for **16** towards Fe<sup>3+</sup> ions were  $5.50 \times 10^{-8}$  M and  $1.69 \times 10^5$  M, respectively. In addition, the reversible fluorescence response to amine/acid vapor of **16** was tested using TLC-based test strip. The real-world application of **16** was tested in natural water sample analysis.

### Mechanistic insights into photophysical properties

Understanding the underlying mechanisms affecting the photophysical properties of the probes is essential for

a comprehensive evaluation of their performance. This section summarizes the three key mechanisms: AIE, TICT, and ESIPT, each of which plays a critical role in the behavior of these probes.

**Aggregation induced emission (AIE).** AIE is a phenomenon where the fluorescence of a probe is significantly enhanced in its aggregated state compared to its dissolved state. This enhancement is due to the restriction of intramolecular motion in the aggregated form, which reduces non-radiative decay pathways and thereby increases fluorescence. For the probes discussed, AIE is particularly relevant in solid or aggregated forms where structural rigidity and intramolecular interactions contribute to enhanced fluorescence. Detailed structural analysis shows that the probes rigid linkers and specific molecular

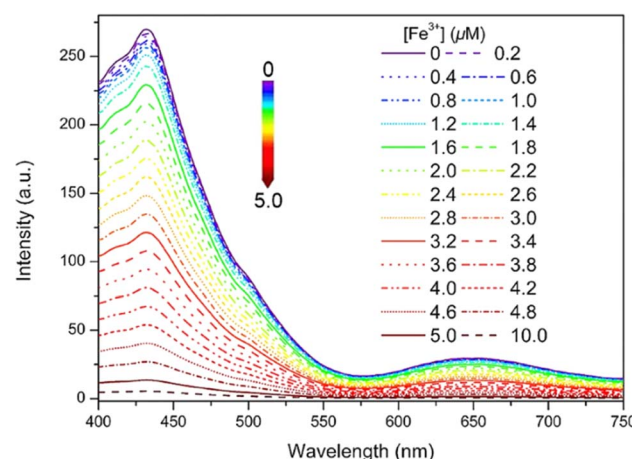


Fig. 22 Emission spectra of probe **16** (10  $\mu$ M) with various concentration of Fe<sup>3+</sup> ions in THF/water mixtures ( $f_w = 90\%$ , pH = 7.4,  $\lambda_{ex} = 380$  nm). Reproduced with permission from ref. 61. Copyright 2024 Elsevier.

arrangements are key factors facilitating AIE. These features help to stabilize the excited state, allowing for a stronger and more efficient emission.

**Twisted intramolecular charge transfer (TICT).** TICT involves the transfer of charge between electron-donating and electron-accepting groups, leading to a twisted molecular conformation in the excited state. This twisting decreases the electronic overlap between donor and acceptor groups, which can significantly influence the emission properties. In the probes, TICT contributes to shifts in emission spectra and broadening of emission bands. The extent of twisting and the nature of the donor-acceptor pairs affect these optical properties. The analysis indicates that TICT is responsible for certain spectral features observed in the probes, highlighting the importance of donor-acceptor interactions and the resulting conformational changes in modulating emission behavior.

**Excited-state intramolecular proton transfer (ESIPT).**<sup>62,63</sup> ESIPT involves the transfer of a proton from a donor site to an acceptor site within a molecule in the excited state. This process can lead to significant changes in emission wavelengths and the appearance of dual emission peaks. For the probes studied, ESIPT influences both emission intensity and color, leading to distinctive spectral characteristics. The presence of functional groups capable of proton transfer and the dynamics of this transfer process are crucial in determining the probes' emission properties. The detailed mechanistic analysis reveals how ESIPT contributes to the observed emission features and offers insights into optimizing probe performance for various applications.

By integrating these mechanistic insights AIE, TICT, and ESIPT into our understanding of the probes' behavior, we gain a comprehensive view of how these processes influence their photophysical properties. This in-depth analysis not only explains the observed phenomena but also provides a foundation for further refinement and application of the probes in detecting metal ions and other sensing tasks.

## Conclusion and future outlook

The detection of metal ions is a crucial task across various domains, including environmental monitoring, biomedical diagnostics, and industrial processes. Schiff bases incorporating cyanostilbene units have emerged as promising probes for this purpose due to their remarkable photophysical properties, structural versatility, and the ability to undergo significant fluorescence changes in the presence of metal ions. This review has provided a comprehensive overview of the synthesis, structural characteristics, and sensing mechanisms of Schiff base-cyanostilbene probes, highlighting their efficacy and potential applications. The incorporation of the cyanostilbene unit into Schiff bases has been shown to enhance the sensitivity and selectivity of these probes towards metal ions. The electron-withdrawing nature of the cyano group in cyanostilbene plays a pivotal role in modulating the electronic properties of the probe, which, in turn, affects its fluorescence response. This unique combination allows for the development of highly responsive and tunable sensors capable of detecting a wide

range of metal ions at low concentrations. The studies reviewed have demonstrated that Schiff base-cyanostilbene probes exhibit excellent selectivity for specific metal ions, such as  $\text{Fe}^{3+}$ ,  $\text{Cu}^{2+}$ ,  $\text{Co}^{2+}$ ,  $\text{Zn}^{2+}$ ,  $\text{Hg}^{2+}$  and other important species including  $\text{ClO}^-$ , arginine, hydrazine and with excellent AIE, TICT characteristics. The coordination interactions with the nitrogen and oxygen atoms of the Schiff base framework led to distinct changes in fluorescence, which can be easily monitored and quantified. Furthermore, the structural diversity of Schiff bases allows for the design of probes with tailored properties to meet specific sensing requirements.

Despite these advancements, several challenges and opportunities remain for future research. A key goal is to further enhance the selectivity and sensitivity of these probes. Modifications to the Schiff base and cyanostilbene structures could enable the detection of a broader range of metal ions at even lower concentrations. Additionally, the development of probes capable of real-time and *in situ* monitoring in complex and dynamic environments such as live tissues and flowing water systems will significantly expand their practical applications. In particular, Schiff base-cyanostilbene probes have shown considerable promise in detecting metal ions in environmental samples, particularly water sources. These probes exhibit high sensitivity and selectivity for harmful metal ions like  $\text{Hg}^{2+}$ ,  $\text{Cu}^{2+}$ , and  $\text{Fe}^{3+}$ , making them valuable tools for monitoring water quality. However, real-world environmental samples often contain a complex mixture of substances that can interfere with probe performance. Matrix effects, such as the presence of organic matter, competing ions, and varying pH levels, can compromise the accuracy and reliability of the probes. Therefore, to overcome these challenges, further optimization is necessary to enhance the selectivity and effectiveness of these probes under diverse environmental conditions. In the field of clinical diagnostics, Schiff base-cyanostilbene probes hold potential for detecting metal ions in biological samples, aiding in diagnosing diseases associated with metal ion imbalances, such as Wilson's disease or iron overload disorders. Despite this potential, the complex biological environment poses significant challenges. Interactions with proteins, lipids, and other biomolecules can lead to false positives or negatives. Therefore, developing probes with enhanced selectivity for target metal ions, even in the presence of complex biological matrices, is crucial for successful clinical applications. Further research should focus on designing probes that can function accurately in the challenging conditions of biological systems. Looking forward, several research directions hold promise for advancing the field of Schiff base-cyanostilbene probes. One exciting area is the development of multifunctional probes capable of simultaneous detection of multiple metal ions, which would allow for comprehensive analysis with a single sensor. Improving probe stability under real-world conditions is also crucial. Research should explore composite materials or hybrid systems to enhance operational stability and effectiveness, ensuring accurate functioning under harsh conditions such as high temperatures, pressures, and varying pH levels. Techniques like encapsulation or protective coatings could also be investigated to prevent probe degradation. Moreover,



optimizing probe design for rapid response times and high sensitivity in dynamic conditions will facilitate continuous monitoring of metal ion levels. Advanced spectroscopic and computational studies will further aid in understanding the fundamental mechanisms of fluorescence changes, leading to more effective sensor designs. Integrating these probes into portable and user-friendly devices will be essential for field applications and clinical diagnostics, making them more accessible for routine monitoring and diagnostic purposes.

In conclusion, Schiff base-cyanostilbene probes represent a highly promising class of sensors for metal ion detection. By addressing current challenges and exploring new research directions, these probes can be further refined and expanded. Future efforts should focus on translating these advancements into practical, reliable sensors for widespread use in environmental monitoring, biomedical diagnostics, and industrial applications. The continued development of Schiff base-cyanostilbene probes holds great promise for enhancing our ability to detect and quantify metal ions, ultimately contributing to improved environmental protection, healthcare, and industrial processes.

## Abbreviations

AIE	Aggregation-induced emission
TICT	Twisted intramolecular charge transfer
ESIPT	Excited-state intramolecular proton transfer
PET	Photoinduced electron transfer
ICT	Intramolecular charge transfer
CHEF	Chelation induced enhanced fluorescence
FRET	Fluorescence resonance energy transfer
nm	Nanometer
nM	Nanomolar
μM	Micromolar
NMR	Nuclear magnetic resonance
HRMS	High-resolution mass spectrometry
FT-IR	Fourier transform infrared
XRD	X-ray diffraction
LOD	Limit of detection
B-H	Benesi-Hildebrand
DFT	Density functional theory
TD-DFT	Time-dependent density-functional theory
ESI-MS	Electrospray ionisation mass spectrometry
WHO	World health organisation
EDTA	Ethylene diamine tetraacetate
AIEE	Aggregation-induced emission enhancement
DMF	Dimethylformamide
PPI	pyrophosphate
UV/PL	UV-vis absorption/photoluminescence
PXRD	Powder X-ray diffraction
THF	Tetrahydrofuran
ppb	Parts per billion
ppm	Parts per million
ns	Nanoseconds
DMSO	Dimethylsulfoxide
ACN	Acetonitrile

## Data availability

No primary research results, software or code have been included and no new data were generated or analysed as part of this review.

## Author contributions

Afrin A.-conceptualization and design of the review, conducted the comprehensive literature search, analyzed and summarized the relevant research, and wrote the initial draft of the manuscript, revised the manuscript for important intellectual content. Chinna Ayya Swamy P.-conceptualization, critical review, editing and finalization. Angel Rose contributed to the preliminary data.

## Conflicts of interest

The authors declare no competing financial interest.

## Acknowledgements

CAS P. thanks, SERB/SRG/2021/002112 for funding and National Institute of Technology for support. Ms. A. A. thanks the National Institute of Technology, Calicut, for the GATE-JRF fellowship.

## References

- 1 X. Zheng, W. Cheng, C. Ji, J. Zhang and M. Yin, *Rev. Anal. Chem.*, 2020, **39**, 231–246.
- 2 K. P. Carter, A. M. Young and A. E. Palmer, *Chem. Rev.*, 2014, **114**, 4564–4601.
- 3 Y. Shen, C. Nie, Y. Wei, Z. Zheng, Z.-L. Xu and P. Xiang, *Coord. Chem. Rev.*, 2022, **469**, 214676.
- 4 M. Patitapaban, B. Rubi, B. Vinita, P. D. Pragyan, K. S. Suban and R. J. Bigyan, *Trends Environ. Anal. Chem.*, 2022, **34**, e00166.
- 5 L. B. Asnake, Gaurav, M. Irshad, K. M. Asho, S. A. Jatinder, K. Vanish and K. Ki-Hyun, *TrAC, Trends Anal. Chem.*, 2019, **116**, 74–91.
- 6 K. G. Manoj, K. P. Goutam and T. Neetu, *Mater. Adv.*, 2022, **3**, 2612–2669.
- 7 M. J. Hafiz, B. Madeeha, W. H. Farah, S. A. Muhammad and S. Nabila, *Crit. Rev. Anal. Chem.*, 2022, **52**, 463–480.
- 8 K. Sikandar, C. Xiaojing, A. Albandary, S. A. Esam, A. A. Fahad, M. I. Munjed and A. Shujat, *J. Environ. Chem. Eng.*, 2021, **9**, 106381.
- 9 U. Duraisamy and V. Inbaraj, *J. Fluoresc.*, 2020, **30**, 1203–1223.
- 10 A. Md Zafer, Alimuddin and A. K. Salman, *J. Fluoresc.*, 2023, **33**, 1241–1272.
- 11 J. Wang, Q. Meng, Y. Yang, S. Zhong, R. Zhang, Y. Fang, Y. Gao and X. Cui, *ACS Sens.*, 2022, **7**, 2521–2536.
- 12 A. Afrin, A. Jayaraj, M. S. Gayathri and P. C. A. Swamy, *Sens. Diagn.*, 2023, **2**, 988–1076.



13 K. Juyal, A. Pathak, M. Panwar, S. C. Thakuri, O. Prakash, A. Agrwal and V. Nand, *J. Organomet. Chem.*, 2023, 122825.

14 A. T. Latha and P. C. A. Swamy, *J. Org. Chem.*, 2024, **89**(12), 8376–8384.

15 A. T. Latha and P. C. A. Swamy, *Chem.–Eur. J.*, 2024, 1841.

16 D. Karati, S. Mukherjee and S. Roy, *Med. Chem.*, 2023, **19**, 960–985.

17 S. Kaushik, S. K. Paliwal, M. R. Iyer and V. M. Patil, *Med. Chem. Res.*, 2023, **32**, 1063–1076.

18 A. Afrin and P. C. A. Swamy, *Coord. Chem. Rev.*, 2023, **494**, 215327.

19 A. Jayaraj, M. S. Gayathri, G. Sivaraman and P. C. A. Swamy P, *J. Photochem. Photobiol. B*, 2022, **226**, 112371.

20 M. K. Goshisht, G. K. Patra and N. Tripathi, *Mater. Adv.*, 2022, **3**, 2612–2669.

21 S. Sasaki, G. P. C. Drummen and G. Konishi, *J. Mater. Chem. C*, 2016, **4**, 2731–2743.

22 E. Zohry, M. Ahmed, E. A. Orabi, M. Karlsson and B. Zietz, *J. Phys. Chem. A*, 2021, **14**, 1252885–1252894.

23 J. Jovaišaitė, P. Baronas, G. Jonusauskas, D. Gudeika, A. Gruodis, J. V. Gražulevičius and S. Juršėnas, *Phys. Chem. Chem. Phys.*, 2023, **25**(3), 2411–2419.

24 L. Zhu and Y. Zhao, *J. Mater. Chem. C*, 2013, **1**, 1059–1065.

25 M. Martínez-Abadía, R. Giménez and M. B. Ros, *Adv. Mater.*, 2018, **30**, 1704161.

26 B. Kumari and S. Kanvah, *Stilbene Stilbene Shining Bright:  $\alpha$ -Cyanostilbenes as Functional Organic Materials*, 2019.

27 J. Luo, Z. Xie, J. W. Y. Lam, L. Cheng, H. Chen, C. Qiu, H. S. Kwok, X. Zhan, Y. Liu, D. Zhu and B. Z. Tang, *Chem. Commun.*, 2001, 1740–1741.

28 J. Mei, N. L. C. Leung, R. T. K. Kwok, J. W. Y. Lam and B. Z. Tang, *Chem. Rev.*, 2015, **21**, 11718–11940.

29 Y. D. Tu, J. Zhang, Y. Zhang, H. H. Y. Sung, L. Liu, R. T. K. Kwok, J. W. Y. Lam, I. D. Williams, H. Yan and B. Z. Tang, *J. Am. Chem. Soc.*, 2021, **143**, 11820–11821.

30 Z. Wang, Y. Zhou, R. Xu, Y. Xu, D. Dang, Q. Shen, L. Meng and B. Z. Tang, *Coord. Chem. Rev.*, 2022, **451**, 214279.

31 Y. Sun, Z. Lei and H. Ma, *J. Mater. Chem. C*, 2022, **10**, 14834–14867.

32 H. Schiff, *J. Am. Chem. Soc.*, 1864, **3**, 343–349.

33 A. L. Berhanu, Gaurav, I. Mohiuddin, A. Malik, A. Singh, V. Kumar and H. Kim, *Trends Anal. Chem.*, 2019, **116**, 74–91.

34 S. Khan, X. Chen, A. Almahri, E. S. Allehyani, F. A. Alhumaydhi, M. M. Ibrahim and S. Ali, *J. Environ. Chem. Eng.*, 2021, **9**, 106381.

35 A. Kumar, M. Saini, B. Mohan and M. Kamboj, *Microchem. J.*, 2022, **181**, 107798.

36 P. Mahalingavelar and S. Kanvah, *Phys. Chem. Chem. Phys.*, 2022, **24**, 23049–23075.

37 Y. H. Chu, C. Y. Zeng, Z. Cao, B. M. Shao, D. H. Li, M. Sun and W. Y. Fang, *Opt. Mater.*, 2023, **139**, 113767.

38 A. Afrin and P. C. A. Swamy, *J. Mater. Chem. C*, 2024, **12**, 1923–1944.

39 A. Afrin and P. C. A. Swamy, *J. Org. Chem.*, 2024, **89**, 7946–7961.

40 A. Afrin and P. C. A. Swamy, *New J. Chem.*, 2023, **47**, 18919–18932.

41 T. Stoerkler, G. Ulrich, A. D. Laurent, D. Jacquemin and J. Massue, *J. Org. Chem.*, 2023, **88**, 9225–9236.

42 T. Yu, P. Theato, H. Yao, H. Liu, Y. Di, Z. Sun and S. Guan, *Chem. Eng.*, 2023, **451**, 138441.

43 X. Yi, X. Liu, Y. Liang, T. Gao, X. Hu and Y. Xiao, *J. Solid State Chem.*, 2024, **334**, 124688.

44 Q. Shi, Y. Ni, L. Yang, L. Kong, P. Gu, C. Wang, Q. Zhang, H. Zhou and J. Yang, *J. Mater. Chem. B*, 2023, **11**, 6859–6867.

45 R. Dahiwadkar, A. Murugan, D. Johnson, R. Chakraborty, V. Thiruvenkatam and S. Kanvah, *J. Photochem. Photobiol. C*, 2023, **434**, 114227.

46 D. Dey, P. Giri, N. Sepay, A. Husain and M. K. Panda, *J. Photochem. Photobiol. A*, 2023, **437**, 114480.

47 G. Zhang, A. Ding, Y. Zhang, L. Yang, L. Kong, X. Zhang, X. Tao, Y. Tian and J. Yang, *Sens. Actuators, B*, 2014, **202**, 209–216.

48 A. Ding, F. Tang, T. Wang, X. Tao and J. Yang, *J. Chem. Sci.*, 2015, **127**, 375–382.

49 G. Zhang, X. Zhang, Y. Zhang, H. Wang, L. Kong, Y. Tian, X. Tao, H. Bi and J. Yang, *Sens. Actuators, B*, 2015, **221**, 730–739.

50 W. Fang, G. Zhang, J. Chen, L. Kong, L. Yang, H. Bi and J. Yang, *Sens. Actuators, B*, 2016, **229**, 338–346.

51 H. Guo, J. Lin, L. Zheng and F. Yang, *Spectrochim. Acta, Part A*, 2021, **256**, 119744.

52 B. Zha, S. Fang, H. Chen, H. Guo and F. Yang, *Spectrochim. Acta, Part A*, 2022, **269**, 120765.

53 Z. Yang, X. Huang, J. Cheng, H. Guo and F. Yang, *Liq. Cryst.*, 2023, **50**, 2521–2528.

54 M. Zhu, M. Zhong, M. Chen, S. Huang, Y. Li and F. Cao, *Opt. Mater.*, 2022, **125**, 112059.

55 S. Huang, L. Zheng, S. Zheng, H. Guo and F. Yang, *J. Photochem. Photobiol. A*, 2022, **427**, 113851.

56 W. Fang, Z. Cao, Q. Liu, Y. Chu, H. Zhu, W. Zhou and J. Yang, *Results Opt.*, 2022, **7**, 100228.

57 M. Chen, W. Huang, Y. Li, Y. Chen, D. Ji and M. Zhu, *Methods Appl. Fluoresc.*, 2022, **11**, 015002.

58 M. Chen, M. Zhong, S. Huang, Y. Chen, F. Cao, H. Hu, W. Huang, D. Ji and M. Zhu, *Inorg. Chem. Commun.*, 2023, **152**, 110640.

59 M. Chen, Y. Chen, M. Zhong, D. Xie, C. Wang, X. Ren, S. Huang, J. Xu and M. Zhu, *J. Fluoresc.*, 2024, **34**, 1075–1090.

60 H. Zhou, X. Huang, S. Zheng, H. Guo and F. Yang, *J. Mol. Struct.*, 2024, **1305**, 137798.

61 M. Chen, W. Chen, Q. Zhu, L. Yang, X. Zhang, D. Xie, J. Chen, Y. Wu, Y. Zhu and M. Zhu, *J. Fluoresc.*, 2024, 1–12.

62 B. Sun, L. Liu, W. Liu, F. Meng and Q. Huang, *J. Lumin.*, 2020, **223**, 117203.

63 U. Duraisamy, P. Jerome, N. Vijay and T. H. Oh, *J. Lumin.*, 2023, 120350.

